Carbon monoxide, a retrograde messenger generated in post-synaptic mushroom body neurons evokes local dopamine release.

Kohei Ueno[1]*, Johannes Morstein[2,3], Kyoko Ofusa[1], Shintaro Naganos[1], Ema Suzuki-Sawano[1], Ayaka Minegishi[4], Hiroaki Kitagishi[4], Christopher J. Chang[2], Junjiro Horiuchi[1], Minoru Saitoe[1]*

[1]Tokyo Metropolitan Institute of Medical Science, 2-1-6 Kamikitazawa, Setagaya-ku, Tokyo, 1568506, Japan.

[2]Departments of Chemistry and Howard Hughes Medical Institute, University of California, Berkeley.

[3]Department of Chemistry, New York University.

[4]Department of Molecular Chemistry and Biochemistry, Faculty of Science and Engineering, Doshisha University, Kyotanabe, Kyoto 610-0321, Japan

*Correspondence to: Kohei Ueno (ueno-kh@igakuken.or.jp), and Minoru Saitoe (saito-mn@igakuken.or.jp)

Dopaminergic neurons innervate extensive areas of the brain and release dopamine (DA) onto a wide range of target neurons. However, DA release is also precisely regulated, and in *Drosophila,* DA is released specifically onto mushroom body (MB) neurons, which have been coincidentally activated by cholinergic and glutamatergic inputs. The mechanism for this precise release has been unclear. Here we found that coincidentally activated MB neurons generate carbon monoxide (CO) which functions as a retrograde signal evoking local DA release from presynaptic terminals. CO production depends on activity of heme oxygenase in post-synaptic MB neurons, and CO-evoked DA release requires Ca^{2+} efflux through ryanodine receptors in DA terminals. Removal of CO using scavengers blocks DA release. We propose that DA neurons utilize two distinct modes of transmission to produce global and local DA signaling.

33 **INTRODUCTION**

34 Dopamine (DA) regulates neural plasticity required for various brain functions (Huang
35 and Kandel, 1995; Molina-Luna et al., 2009; Yagishita et al., 2014). Consistent with
36 their roles in regulating global brain states including arousal and mood, individual DA
37 neurons innervate extensive areas of the brain and release DA onto a wide range of
38 target neurons through a processes known as volume transmission (Agnati et al., 1995;
39 Matsuda et al., 2009; Rice and Cragg, 2008). However, this extensive innervation is not
40 suitable for precise, localized release of DA. Therefore, it has been unclear whether and
41 how DA-dependent plastic changes are directed to specific target neurons.

42 A recent *Drosophila* study identified synaptic vesicular (SV) exocytosis from DA
43 terminals that is restricted to mushroom body (MB) neurons that have been activated by
44 coincident inputs from two different cholinergic and glutamatergic sensory pathways
45 (Ueno et al., 2017). *Drosophila* mushroom bodies (MBs) receive odor and
46 somatosensory information, and form associations between these two inputs during
47 olfactory associative learning. Information regarding odors is transmitted to the MB by
48 projection neurons (PNs) from the antennal lobe (AL), while somatosensory
49 information from the body is transmitted to the brain via ascending fibers of the ventral
50 nerve cord (AFV). AL stimulation evokes Ca^{2+} responses in the MB by activating
51 nicotinic acetylcholine receptors (nAChRs), and AFV stimulation evokes Ca^{2+}
52 responses in the MBs by activating NMDA receptors (NRs) in the MBs (Ueno et al.,
53 2013). Significantly, when the AL and AFV are stimulated simultaneously (AL + AFV)
54 or the AL and NRs are stimulated simultaneously (AL + NMDA), plasticity occurs such
55 that subsequent AL stimulations cause an increase in Ca^{2+} responses in the MB (Ueno et
56 al., 2013; Wang et al., 2008). This plasticity is known as long-term enhancement (LTE)

57 of MB responses and requires activation of D1 type DA receptors (D1Rs) in the MBs.
58 Furthermore, while activation of D1Rs alone is sufficient to produce LTE, neither AL
59 nor AFV stimulation alone is able to cause SV exocytosis from presynaptic DA
60 terminals. Instead, exocytosis from DA terminals occurs only when postsynaptic MB
61 neurons are activated by coincident AL + AFV or AL + NMDA stimulation. Strikingly,
62 while MBs are bilateral structures and DA neurons project terminals onto both sides of
63 MBs (Mao and Davis, 2009), SV exocytosis occurs specifically in MB areas that have
64 been coincidently activated. Based on these results, we proposed that coincident inputs
65 specify the location where DA is released, while DA induces plastic changes needed to
66 encode associations. However, it has been unclear how coincidentally activated MB
67 neurons induce SV exocytosis from presynaptic DA terminals. Locally restricted SV
68 exocytosis upon coincident activation of MB neurons requires activity of the *rutabaga*
69 type of adenylyl cyclase, which is proposed to be a coincident detector in the MBs.
70 Thus it has been proposed that MB neurons sense coincident activation and send a
71 retrograde "demand" signal to presynaptic terminals to evoke local DA release (Ueno et
72 al., 2017).

73 In this study, we used a *Drosophila* dissected brain system to examine synaptic
74 plasticity and DA release, and found that coincidentally activated post-synaptic MB
75 neurons generate the retrograde messenger, carbon monoxide (CO). CO is generated by
76 heme oxygenase (HO) in post-synaptic MB neurons, and induces DA release from
77 pre-synaptic terminals by evoking Ca^{2+} release from internal stores via ryanodine
78 receptors (RyRs). Thus, while individual DA neurons extensively innervate the MBs,
79 on-demand SV exocytosis allows DA neurons to induce plasticity in specific target
80 neurons.

81

82 **RESULTS**

83

84 **CO synthesis in the MB neurons is required for DA release upon coincident**
85 **stimulation**

86 Previously, we used an *ex vivo* dissected brain system to examine SV exocytosis from
87 DA terminals projecting onto the tips of the vertical lobes of the MBs. We measured SV
88 exocytosis from DA terminals using a vesicular exocytosis sensor, synapto-pHluorin
89 (spH) (Miesenbock et al., 1998), expressed in dopaminergic neurons using a tyrosine
90 hydroxylase (TH) driver, and found that release occurred only upon coincident
91 activation of post-synaptic MB neurons by cholinergic inputs from the ALs and
92 glutamatergic inputs from the AFV (Ueno et al., 2017). To verify this result, we
93 currently utilized a fluorescent substrate of the vesicular monoamine transporter
94 (VMAT), FFN511, which selectively accumulates in DA vesicles in DA neurons
95 (Pereira et al., 2016). FFN511 is released along with DA upon SV exocytosis, reducing
96 fluorescence. Using FFN511, we confirmed that SV exocytosis from TH-DA terminals
97 on the tip of vertical lobes of the MB did not occur upon either 200 μM NMDA or AL
98 stimulation alone, but did occur upon coincident AL and 200 μM NMDA stimulation
99 (Figure **S1A**).

100 If postsynaptic MB activity evokes SV exocytosis from presynaptic DA terminals,
101 vesicular output from MB neurons may be needed to activate DA neurons that loop
102 back to the MBs, as suggested in previous studies (Cervantes-Sandoval et al., 2017;
103 Ichinose et al., 2015; Takemura et al., 2017). Alternatively, a retrograde message may be
104 released from MB neurons to regulate pre-synaptic release. To test these possibilities,

105 we first inhibited synaptic transmission from MB neurons by expressing
106 temperature-sensitive *shi*^{ts} from a pan-MB driver, *MB-LexA*. Recall of olfactory
107 memory is disrupted by inhibiting synaptic outputs from MBs during retrieval (Dubnau
108 et al., 2001; McGuire et al., 2001). Similarly, we found that recall of olfactory memory
109 was disrupted at restrictive temperature in *MB-LexA>LexAop-shi*^{ts} flies (Figure **S1B**),
110 confirming that MB synaptic output is blocked at restrictive temperature in these flies.
111 However, SV exocytosis from TH-DA terminals occurs normally in these flies upon
112 coincident AL + NMDA stimulation at restrictive temperature (Figure **1A**), suggesting
113 that vesicular output from MB is not necessary for DA release. SV exocytosis from
114 TH-DA terminals also occurred normally when *shi*^{ts} was expressed using a different MB
115 driver (*c747-GAL4>UAS-shi*^{ts}) (Figure **S1C**), even though memory recall is also
116 disrupted at restrictive temperature in this line (Dubnau et al., 2001). 1 mM 1-octanol, a
117 blocker of gap junctional communication (Goncharenko et al., 2014; Rorig et al., 1996),
118 also did not inhibit SV exocytosis in TH-DA terminals (Figure **1B**). These results
119 suggest that output from chemical and electrical synapses is not required for the MBs to
120 induce DA-release from DA neurons. We next examined whether the retrograde
121 messenger, nitric oxide (NO), may mediate SV exocytosis in TH-DA terminals.
122 However, 100 μM L-NAME (Nϖ-L-nitro arginine methyl ester), a NO synthetase
123 blocker (Boultadakis and Pitsikas, 2010) had no effect on AL + NMDA
124 stimulation-induced SV exocytosis from TH-DA terminals (Figure **1C**).

125 Since DA release is critical for forming associations between AL and AFV inputs,
126 mutations that affect a demand signal for DA release should be detrimental for olfactory
127 aversive learning. Olfactory memory is disrupted by mutations in *nemy*, a gene that
128 encodes a *Drosophila* homolog of cytochrome B561 (CytB561) (Iliadi et al., 2008).

129 CytB561 is involved in metabolism of carbon monoxide (CO) (Cypionka and Meyer,
130 1983; Jacobitz and Meyer, 1989; Sugimura et al., 1980), a diffusible gas similar to NO,
131 that has been proposed to act as a retrograde messenger during synaptic plasticity
132 (Alkadhi et al., 2001; Shibuki et al., 2001). Thus we next examined whether CO may be
133 required for DA release. CO is synthesized by heme oxygenase (HO), and we found that
134 SV exocytosis from TH-DA terminals to coincidentally activated MB neurons was
135 abolished upon application of chromium mesoporphyrin (CrMP), a HO blocker
136 (Vreman et al., 1993) (Figure **1D**). Consistent with the requirement of DA release for
137 plasticity, LTE was also significantly inhibited by CrMP (Figure **S2A**). When we
138 examined the *Drosophila* homologue of HO (dHO) (Cui et al., 2008) using anti-dHO
139 antibodies, we found that dHO was expressed strongly in the MBs and in insulin
140 producing cells (Figure **S2B**). To determine whether dHO in the MBs is required for
141 DA release, we used an RU486-inducible *MB247-switch* (*MBsw*) driver (Mao et al.,
142 2004) to express a *dHO-RNAi* construct (*MBsw>UAS-dHO-IR*), and found that SV
143 exocytosis from TH-DA terminals was impaired in flies fed RU486 (Figure **1E and**
144 **Movie S1**). Likewise, LTE was also significantly inhibited in brains from
145 *MBsw>UAS-dHO-IR* flies treated with RU486 (Figure **S2C**). Furthermore, acute knock
146 down of dHO in the MBs in *MBsw>UAS-dHO-IR* flies disrupted olfactory memory
147 (Figure **S2D**) without affecting task-related responses (Figure **S2E**). Altogether, these
148 results indicate that dHO is required for olfactory memory, MB plasticity, and DA
149 release onto MBs.
150
151 **CO generated from coincidentally activated MB neurons evokes DA release**

152 To examine whether CO can directly induce SV exocytosis from DA terminals, we
153 applied CO-saturated saline from micropipettes to the vertical lobes of the MBs, and
154 observed robust SV exocytosis from TH-DA terminals (Figure **2A**). Furthermore, we
155 found that application of CO-releasing molecule-3 (CORM-3), a water-soluble
156 CO-donor (Aki et al., 2018; Tinajero-Trejo et al., 2014), also evokes SV exocytosis
157 from TH-DA terminals (Figure **2B**). In contrast, application of other retrograde
158 messengers, including 200 μM arachidonic acid and 200 μM 2-arachidonylglycerol, an
159 endocanabinoid receptor agonist, had no effects on release (Figure **2C** and **2D**).

160 To next visualize the generation and release of CO from MB neurons we used a CO
161 selective fluorescent probe, CO Probe 1 (COP-1) (Michel et al., 2012). While COP-1
162 fluorescence increased immediately after coincident AL + NMDA stimulation,
163 fluorescence remained unchanged after AL stimulation or NMDA application alone
164 (Figure **3A**). Thus, changes in COP-1 fluorescence parallel changes in DA release.
165 Furthermore, the fluorescence increase in COP-1 occurred on the lobes of the MBs
166 ipsilateral, but not contralateral, to the stimulated AL (Figure **3B and Movie S2**). Since
167 each AL innervates its ipsilateral, but not contralateral MB, this result indicates that CO
168 production occurs only in areas of coincident AL and NMDA activation. Again this
169 result parallels results for DA release (Ueno et al., 2017). Significantly, increased
170 COP-1 fluorescence was attenuated by knocking down dHO in the MBs (Figure **3C**),
171 indicating that COP-1 detects CO, and CO production requires dHO.

172 HO generates CO by catalyzing the breakdown of heme into biliverdin, ferrous iron,
173 and CO (Tenhunen et al., 1969). Thus, biliverdin or its metabolite, bilirubin, may also
174 function in DA release. To test whether endogenously generated CO per se evokes
175 release, we used a CO selective scavenger, hemoCD (Kitagishi et al., 2010). In the

176 presence of hemoCD, exocytosis from TH-DA terminals upon AL + NMDA stimulation
177 was significantly inhibited (Figure 3D), indicating that CO is required for release.
178 Collectively, these results suggest that coincident stimulation of MB neurons induces
179 dHO to generate the retrograde messenger, CO, which then evokes SV exocytosis from
180 presynaptic DA terminals.
181
182 **CO evokes non-canonical SV exocytosis**
183 SV exocytosis requires an increase in Ca^{2+} concentration in presynaptic terminals
184 (Augustine et al., 1985; Katz and Miledi, 1967; Meinrenken et al., 2003; Sabatini and
185 Regehr, 1996). Consistent with this, we observed a robust Ca^{2+} increase in TH-DA
186 terminals that project onto the MB lobes receiving coincident AL + NMDA stimulation
187 (Figure 4A), but not in TH-DA terminals that project onto the contralateral side (Figure
188 4B). Ca^{2+} increases in DA terminals were also observed upon application of CORM-3
189 (Figure 4C), and this increase was abolished by addition of the membrane-permeable
190 Ca^{2+} chelator BAPTA-AM (Figure 4D). In canonical SV exocytosis, neuronal activity
191 opens voltage-gated calcium channels, allowing influx of extracellular Ca^{2+} (Augustine
192 et al., 1985; Katz and Miledi, 1967). However, we found that CORM-3 is able to induce
193 SV exocytosis from TH-DA terminals even in Ca^{2+} free saline in the presence of the
194 Ca^{2+} chelator, EGTA, and the sodium channel blocker, TTX (Figure 4E). This suggests
195 that CO-evoked DA release is action potential independent and does not require Ca^{2+}
196 influx from extracellular sources.
197 Since extracellular Ca^{2+} is not responsible for CO-dependent DA release, we next
198 examined whether Ca^{2+} efflux from internal stores may be required. Significantly,
199 CORM-3 failed to increase Ca^{2+} in TH-DA terminals in the presence of EGTA and

200 thapsigargin, an inhibitor of the sarcoplasmic/endoplasmic reticulum Ca^{2+} ATPase
201 (SERCA), which depletes internal Ca^{2+} stores (Kijima et al., 1991; Sagara and Inesi,
202 1991) (Figure **4F**). Thus, CO-evoked DA release occurs through a non-canonical
203 mechanism that depends on Ca^{2+} efflux from internal stores rather than from
204 extracellular sources.
205
206 **Ryanodine receptors mediate Ca^{2+} efflux for CO-evoked DA release.**
207 What mediates Ca^{2+} efflux from internal stores in DA terminals? Inositol
208 1,4,5-trisphosphate receptors (IP_3Rs) and ryanodine receptors (RyRs) are the major
209 channels mediating Ca^{2+} release from internal stores (Bardo et al., 2006). While SV
210 exocytosis evoked by coincident MB stimulation was not suppressed by
211 2-Aminoethoxydiphenyl borate (2-APB), an IP_3R antagonist (Maruyama et al., 1997)
212 (Figure **5A**), exocytosis was significantly inhibited by dantrolene, a RyR antagonist
213 (Zhao et al., 2001) (Figure **5B**). Conversely, application of a RyR agonist,
214 4-chloro-3-methylphenol (4C3MP) (Zorzato et al., 1993) was sufficient to evoke
215 exocytosis (Figure **5C**). These data suggest that RyRs in DA neurons are required for
216 SV exocytosis upon coincident activation of MB neurons.
217 To address whether RyRs are expressed in DA terminals, we examined expression of
218 mCD8::GFP in *Mi{Trojan-GAL4.0}RyR*$^{MI08146\text{-}TG4.0}$*; P{UAS-mCD8::GFP}* flies. In
219 *Mi{Trojan-GAL4.0}RyR*$^{MI08146\text{-}TG4.0}$, a Trojan GAL4 exon is inserted between exons 18
220 and 19 in the same orientation as the RyR gene (Diao et al., 2015). Thus GAL4, and
221 mCD8::GFP, expression should reflect RyR expression. In these flies, mCD8::GFP
222 signals overlapped with anti-TH antibody signals, indicating that RyRs are expressed in
223 DA neurons (Figure **S3A**). To determine whether RyRs in the DA terminals are required

224 for DA release, we knocked down RyRs in TH-DA neurons and examined release upon
225 AL + NMDA stimulation. SV exocytosis from DA terminals was significantly
226 suppressed by knocking down RyRs (Figure **5D**). Furthermore, knocking down RyRs in
227 TH-DA neurons also suppressed SV exocytosis induced by direct CO application to
228 TH-DA terminals (Figure **5E**). Knocking down of RyRs in TH-DA neurons also
229 impaired short-term olfactory memory (Figure **S3B**) without affecting odor and shock
230 response (Figure **S3C**), and suppressed LTE upon coincident AL + NMDA stimulation
231 (Figure **S3D**). Thus, pre-synaptic RyRs are required for CO and coincident activation
232 dependent DA release, MB plasticity, and olfactory memory.
233

234 DISCUSSION

235

236 CO functions as a retrograde on-demand messenger for SV exocytosis in 237 presynaptic DA terminals

238 A central tenet of neurobiology is that action potentials, propagating from the cell
239 bodies, induce Ca^{2+} influx in presynaptic terminals to evoke SV exocytosis. However,
240 recent mammalian studies have shown that only a certain fraction of a large number of
241 pre-synaptic release sites is involved in canonical SV exocytosis (Liu et al., 2018;
242 Pereira et al., 2016). In this study we identify a novel mechanism of SV exocytosis in
243 which activity in post-synaptic neurons evokes pre-synaptic release to induce plastic
244 changes. This mechanism allows the timing and location of DA release to be strictly
245 defined by activity of postsynaptic neurons.

246 On-demand SV exocytosis utilizes CO as a retrograde signal from postsynaptic MB
247 neurons to presynaptic DA terminals. We demonstrate that CO fulfills the criteria that

248 have been proposed for a retrograde messenger (Regehr et al., 2009). First, we
249 demonstrate that HO, which catalyzes CO production, is highly expressed in
250 postsynaptic MB neurons, indicating that MB neurons have the capacity to synthesize
251 the messenger. Second, we show that pharmacological and genetic suppression of HO
252 activity in the MBs inhibits CO production, pre-synaptic DA release, and LTE. Third,
253 using a CO fluorescent probe, COP-1 (Michel et al., 2012), we demonstrate that CO is
254 generated in the MBs following coincident stimulation of the MBs, and CO generation
255 is restricted to lobes of MB neurons that receive coincident stimulation. We further
256 show that direct application of CO, or a CO donor, induces DA release from presynaptic
257 terminals, while addition of a CO scavenger, HemoCD, suppresses release. Fourth, we
258 demonstrate that CO activates RyRs in presynaptic terminals to induce SV exocytosis.
259 Strikingly, CO-dependent SV exocytosis does not depend on influx of extracellular Ca^{2+},
260 but instead requires efflux of Ca^{2+} from internal stores via RyRs. Finally, we show that
261 pharmacological inhibition and genetic suppression of RyRs in DA neurons impairs DA
262 release after coincident stimulation and CO application.

263 While other retrograde signals, such as NO and endo cannabinoids enhance or
264 suppress canonical SV exocytosis, we find that CO-dependent DA release occurs even
265 in conditions which block neuronal activity and Ca^{2+} influx in presynaptic DA terminals.
266 This suggests that CO does not function to modulate canonical SV exocytosis, but may
267 instead evoke exocytosis through a novel mechanism. Several previous studies have
268 indicated that CO and RyR-dependent DA release also occurs in mammals. A
269 microdialysis study has shown that CO increases the extracellular DA concentration in
270 the rat striatum and hippocampus (Hiramatsu et al., 1994), either through increased DA
271 release, or inhibition of DA reuptake (Taskiran et al., 2003). Also, pharmacological

272 stimulation of RyRs has been reported to induce DA release in the mice striatum
273 (Oyamada et al., 1998; Wan et al., 1999). This release is attenuated in RyR3 deficient
274 mice, while KCl-induced DA release, which requires influx of extracellular Ca^{2+}, is
275 unaffected, suggesting that RyR-dependent release is distinct from canonical DA release.
276 However, it has been unknown whether and how CO is generated endogenously. Also
277 physiological conditions that activate RyRs to evoke DA release have also been unclear.
278

279 **Signaling pathway for CO-dependent on-demand release of DA**

280 While most neurotransmitters are stored in synaptic vesicles and released upon neuronal
281 depolarization, the release of gaseous retrograde messengers such as NO and CO is
282 likely coupled to activation of their biosynthetic enzymes, NOS and HO. Previously, we
283 demonstrated that activity-dependent DA release onto the MBs requires *rutabaga*
284 adenylyl cyclase (*rut*-AC) in the MBs (Ueno et al., 2017). *rut*-AC is proposed to
285 function as a neuronal coincidence detector that senses coincident sensory inputs and
286 activates the PKA pathway by increasing production of cAMP. In mammals, activation
287 of the cAMP/PKA pathway increases expression of an HO isoform, HO-1, through
288 transcriptional activation of the transcription factor CREB (Astort et al., 2016; Durante
289 et al., 1997; Park et al., 2013). However, gene expression changes are not fast enough to
290 explain CO-dependent DA release. A second mammalian HO isoform, HO-2 is
291 selectively enriched in neurons, and HO-2-derived CO is reported to function in
292 plasticity. HO-2 is activated by Ca^{2+}/calmodulin (CaM) binding (Boehning et al., 2004),
293 and by casein kinase II (CKII) phosphorylation (Boehning et al., 2003), two
294 mechanisms that can generate CO with sufficient speed to account for LTE. Currently, it
295 is unclear whether *rut*-AC and the cAMP/PKA pathway functions in parallel with

296 Ca^{2+}/CaM and CKII, or in concert with these pathways (ie functions as a priming kinase
297 for CKII (Huang et al., 2007)) to activate HO. Supporting the concept that PKA
298 regulates HO, in the golden hamster retina, PKA has been shown to increase HO
299 activity without affecting HO gene expression (Sacca et al., 2003).

300 While *Drosophila* has a single isoform of RyR, mammals have three isoforms, RyR1
301 to RyR3. Skeletal muscle and cardiac muscle primarily express RyR1 and RyR2, and
302 the brain, including the striatum, hippocampus and cortex, expresses all three isoforms
303 (Giannini et al., 1995). RyRs are known to be activated by Ca^{2+} to mediate Ca^{2+} induced
304 Ca^{2+} release (CICR) (Endo, 2009). However, CO-evoked DA release occurs even in the
305 presence of Ca^{2+}-free extracellular solutions containing TTX and EGTA, suggesting that
306 CO activates RyRs through a different mechanism. Besides Ca^{2+}, RyRs can be activated
307 by calmodulin, ATP, PKA, PKG, cADP-ribose, and NO (Kakizawa, 2013; Lanner et al.,
308 2010; Takasago et al., 1991; Verkhratsky, 2005; Xu et al., 1998; Zalk et al., 2007). NO
309 can directly stimulate RyR1 non-enzymatically by S-nitrosylating a histidine residue to
310 induce Ca^{2+} efflux (Kakizawa, 2013; Xu et al., 1998). Similarly, CO has been reported
311 to activate Ca^{2+}-activated potassium channels (K_{Ca}) through a non-enzymatic reaction in
312 rat artery smooth muscle (Wang and Wu, 2003). Alternatively, both NO and CO can
313 bind to the heme moiety of soluble guanlylate cyclase (sGC) leading to its activation
314 (Stone and Marletta, 1994). Activated sGC produces cGMP, and cGMP-dependent
315 protein kinase (PKG) rapidly phosphorylates and activates RyRs (Takasago et al., 1991).
316 Interestingly, NO increases DA in the mammalian striatum in a neural activity
317 independent manner (Hanbauer et al., 1992; Lonart et al., 1993; Zhu and Luo, 1992).
318 Since activation of RyRs also increases extracellular DA in the striatum, hippocampus
319 and cortex (Oyamada et al., 1998; Wan et al., 1999), NO may play a pivotal role in RyR

320 activation and DA release in mammals. However, NOS expression has not been
321 detected in the MBs (Muller, 1994; Regulski and Tully, 1995), suggesting that in
322 *Drosophila*, CO rather than NO may function in this process.
323
324 **Biological significance of on-demand DA release**
325 DA plays a critical role in associative learning and synaptic plasticity (Huang and
326 Kandel, 1995; Jay, 2003; Lee et al., 2016; Puig et al., 2014; Yamasaki and Takeuchi,
327 2017). In flies, neutral odors induce MB responses by activating sparse subsets of MB
328 neurons. After being paired with electrical shocks during aversive olfactory
329 conditioning, odors induce larger MB responses in certain areas of the MBs (Akalal et
330 al., 2011; Davis, 2011; Wang et al., 2008; Yu et al., 2006). We modeled this plastic
331 change in *ex vivo* brains as LTE, and showed that DA application alone is sufficient to
332 induce this larger response (Ueno et al., 2017). However, in the *Drosophila* brain, only a
333 small number of DA neurons (~12 for aversive and ~100 for appetitive) regulate
334 plasticity in ~2000 MB Kenyon cells (Mao and Davis, 2009). Thus to form
335 odor-specific associations, there should be a mechanism regulating release at individual
336 synapses. CO-dependent on-demand DA release provides this type of control. If
337 on-demand release is involved in plasticity and associative learning, knockdown of
338 genes associated with release should affect learning. Indeed, we show that knocking
339 down either dHO in the MBs or RyRs in DA neurons impairs olfactory conditioning.
340 While these knockdowns did not completely abolish olfactory conditioning, this may be
341 due to inefficiency of our knockdown lines. Alternatively, on-demand release may not
342 be the only mechanism responsible for memory formation, but may instead be required
343 for a specific phase of olfactory memory.

344 In mammals, the role of CO in synaptic plasticity is unclear. Application of CO
345 paired with low frequency stimulation induces LTP, while inhibiting HO blocks LTP in
346 the CA1 region of the hippocampus (Zhuo et al., 1993). However, HO-2 deficient mice
347 have been reported to have normal hippocampal CA1 LTP (Poss et al., 1995). In
348 contrast to CO, a role for NO in synaptic plasticity and learning has been previously
349 reported (Balaban et al., 2014; Korshunova and Balaban, 2014; Muller, 1996). Thus, at
350 this point it is an open question whether CO or NO evokes DA release in mammals.
351 Downstream from CO or NO, RyRs have been shown to be required for hippocampal
352 and cerebellum synaptic plasticity (Balschun et al., 1999; Kakizawa et al., 2012; Lu and
353 Hawkins, 2002; Wang et al., 1996).
354 Our current results suggest that DA neurons release DA via two distinct mechanisms:
355 canonical exocytosis and on-demand release. Canonical exocytosis is evoked by
356 electrical activity of presynaptic DA neurons, requires Ca^{2+} influx, and may be involved
357 in volume transmission. This mode of release can activate widespread targets over time,
358 and is suited for regulating global brain functions. In contrast, on-demand release is
359 evoked by activity of postsynaptic neurons, requires Ca^{2+} efflux via RyRs, and can
360 regulate function of specific targets at precise times. DA neurons may differentially
361 utilize these two modes of SV exocytosis in a context dependent manner. Understanding
362 how DA neurons differentially utilize these modes of transmission will provide new
363 insights into how a relatively small number of DA neurons can control numerous
364 different brain functions.
365
366 **EXPERIMENTAL PROCEDURES**
367

368 **Fly Stock maintenance**

369 All fly stocks were raised on standard cornmeal medium at 25 ± 2˚C and 60 ± 10%
370 humidity under a 12/12 h light–dark cycle. Flies were used for experiments 1-3 d after
371 eclosion.

372

373 **Transgenic and mutant lines**

374 All transgenic and mutant lines used in this study are listed in supplemental Table S1.
375 *UAS-G-CaMP3* (BDSC_32234, Bloomington Stock Center, Indiana),
376 *LexAop-G-CaMP2* (Ueno et al., 2013) and *LexAop-R-GECO1* lines were used for
377 measuring Ca^{2+} responses as described previously (Ueno et al., 2013).
378 *UAS-synapto-pHluorin* (*UAS-spH*) (Ng et al., 2002) and *LexAop-synapto-pHluorin*
379 (*LexAop-spH*) lines were used for measuring vesicle release (Ueno et al., 2013).
380 *MB-LexA::GAD* (Ueno et al., 2013) was used for the *LexA* MB driver, *c747* (Aso et al.,
381 2009) was used as the *GAL4* MB driver, and *TH-GAL4* (Friggi-Grelin et al., 2003) and
382 *TH-LexAp65* (Ueno et al., 2013) were used for *TH-DA* drivers. *UAS-shi^{ts}* (Kitamoto,
383 2001) and *pJFRC104-13XLexAop2-IVS-Syn21-Shibire-ts1-p10* (*LexAop-shi^{ts}*) (Pfeiffer
384 et al., 2012) lines were used for inhibition of synaptic transmission. *MB247-Switch*
385 (*MBsw*) was used to express a *UAS* transgene in the MBs upon RU486 (RU+) feeding
386 for 3-5 days (Mao et al., 2004). *UAS-dHO IR* was used to knockdown of *dHO*
387 expression (Cui et al., 2008). *dHO$^{\Delta}$* is a deficiency line *Df(3R)Exel7309* (BDSC 7960),
388 lacking 65 Kbp including *dHO* (Flybase; http://flybase.org) in the third chromosome.
389 *P{KK101716}VIE-260B* (VDRC ID 109631, Vienna Drosophila Resource Center,
390 Vienna, Austria) (*UAS-RyR RNAi*) was used to knock down *RyR*.
391 *Mi{Trojan-GAL4.0}RyR[MI08146-TG4.0]* (BDSC 67480) carries a *GAL4* sequence

392 between 18 and 19 exon of *RyR* and was used to monitor *RyR* gene expression.

393

394 **Isolated whole brain preparation**

395 Brains were prepared for imaging as previously described (Ueno et al., 2013). Briefly,
396 brains were dissected in ice cold 0 mM Ca^{2+} HL3 medium (in mM, NaCl, 70; sucrose,
397 115; KCl, 5; $MgCl_2$, 20; $NaHCO_3$, 10; trehalose, 5; Hepes, 5; pH 7.3) (Stewart et al.,
398 1994), and placed in a recording chamber filled with normal, room temperature HL3
399 medium (the same recipe as above, containing 1.8 mM $CaCl_2$). To deliver hemoCD
400 through the blood brain barrier, brains were treated with papain (10 U/ml) for 15 min at
401 room temperature, and washed several times with 0 mM Ca^{2+} HL3 medium prior to use
402 (Gu and O'Dowd, 2007; Ueno et al., 2017).

403

404 **Imaging analysis**

405 Imaging analysis was performed as described previously (Ueno et al., 2013; Ueno et al.,
406 2017). Briefly, fluorescent images were captured at 15 Hz using a confocal microscope
407 system (A1R, Nikon Corp., Tokyo, Japan) with a 20x water-immersion lens (numerical
408 aperture 0.5; Nikon Corp). We obtained F_0 by averaging the 5 sequential frames before
409 stimulus onset and calculated $\Delta F/F_0$. To evaluate stimulation-induced fluorescent
410 changes of spH, $\Delta F/F_0$ calculated in the absence of stimulation or pharmacological
411 agents was subtracted from stimulus or drug induced $\Delta F/F_0$. To quantitatively evaluate
412 the spH fluorescent changes, the average values of fluorescent changes at indicated time
413 points during and after stimulation were statistically compared.

414 The AL was stimulated (30 pulses, 100 Hz, 1.0 ms pulse duration) using glass
415 micro-electrodes. For NMDA stimulation, 200 μM NMDA, diluted in HL3 containing 4

416 mM Mg^{2+} (Miyashita et al., 2012), was applied by micro pipette.

417 For application of CO-saturated HL3, CO or control N_2 gas was dissolved in HL3
418 saline by bubbling. CO or N_2 saturated solutions were immediately placed in glass
419 pipettes and puffed onto the MB lobes for 1 min (pressure = 6 psi) using a Picospritzer
420 III system (Parker Hannifin Corp., USA). While we first used thin tip micropipettes,
421 approximately 5 micro m diameter (Figure. 2A), we also used larger tip micropipettes,
422 approximately 15 micro m (Figure 5E), to avoid clogging.

423 To measure SV exocytosis using FFN511, *MB-LexA:GAD, LexAop-R-GECO1* brains
424 were incubated in 10 μM FFN511/HL3 for 30 min. To remove non-specific binding of
425 the dye, FFN511 loaded brains were washed in 200 μM ADVASEP-7/HL3 for 15 min
426 two times (Gubernator et al., 2009; Kay et al., 1999). To evaluate stimulation-induced
427 release of FFN511, $\Delta F/F_0$ in the absence of stimulation was subtracted from $\Delta F/F_0$

428

429 **Behaviors**

430 Olfactory aversive memory: The procedure for measuring olfactory memory has been
431 previously described (Tamura et al., 2003; Tully and Quinn, 1985). Briefly, two mildly
432 aversive odors (3-octanol [OCT]) or 4-methylcyclohexanol [MCH]) were sequentially
433 delivered to approximately 100 flies for 1 min with a 45 sec interval between each odor
434 presentation. When flies were exposed to the first, CS^+ odor (either OCT or MCH), they
435 were also subjected to 1.5 sec pulses of 60 V DC electric shocks every five sec. To test
436 olfactory memory, flies were placed at the choice point of a T-maze where they were
437 allowed to choose either the CS+ or CS- odor for 1.5 min. Memory was calculated as a
438 performance index (PI), such that a 50:50 distribution (no memory) yielded a
439 performance index of zero and a 0:100 distribution away from the CS^+ yielded a

440 performance index of 100.

441

442 Odor and Shock avoidance. Peripheral control experiments including odor and shock
443 reactivity assays were performed as previously described (Tully and Quinn, 1985) to
444 measure sensitivity to odors and electrical shocks. Approximately 100 flies were placed
445 at the choice point of a T maze where they had to choose between an odor (OCT or
446 MCH) and mineral oil or between electrical shocks and non-shocked conditions. A
447 preformance index was calculated as described above.

448

449 **Identification of dHO localization**

450 To detect of dHO protein in fly brains, wild-type, w(CS) (Dura et al., 1993), and *dHO*$^{\Delta}$
451 flies were dissected and fixed in 4 % paraformaldehyde for 20 min at 4°C. Brains were
452 incubated in PBS with 5 % FBS and 0.1 % Triton-X for 30 min at 4°C, and then in
453 primary antibodies, 1:50 anti-HO (Cui et al., 2008) and 1:20 anti-Fas2 (1D4,
454 Developmental Studies Hybridoma Bank, Iowa, USA) for 3 days at 4°C. After washing,
455 brains were incubated with secondary antibodies, Alexa488-conjugated donkey anti-rat
456 antibody (1:200) (Invitrogen, Carlsbad, USA) and Alexa555-conjugated donkey
457 anti-mouse antibody (1:200) (Invitrogen) for 2 days at 4°C. Images were captured using
458 an A1R confocal microscope (Nikon, Tokyo, Japan).

459

460 **Identification of RyR positive neurons (Trojan)**

461 For *Mi{Trojan-GAL4.0}RyR[MI08146-TG4.0]/UAS-mCD8::GFP* imaging, heads were
462 dissected in 4 % paraformaldehyde for 30 min at 4°C. Brains were incubated with
463 primary antibodies, anti-GFP (1:400) (ab13970, Abcam, Cambridge, UK) and

464 anti-tyrosine hydroxylase (#22941, Immunostar, Hudson, USA) in PBS with 10 %
465 ImmunoBlock (DS Pharma Biomedical Co., Osaka, Japan) and 0.1 % Triton-X
466 overnight at 4°C. After washing, brains were incubated with secondary antibodies,
467 Alexa488-conjugated donkey anti-chick antibody (1:400) (Jackson ImmunoResearch,
468 West Grove, USA) and Alexa555-conjugated donkey anti-mouse antibody (1:400)
469 (Invitrogen) overnight at 4°C. Images were captured using an A1R confocal microscope
470 (Nikon, Tokyo, Japan).
471
472 **Chemicals and treatments**
473 RU486 (mifepristone), NMDA (N-methyl-D-aspartate), L-NAME (Nϖ-L-nitro arginine
474 methyl ester), 1-octanol, 2-arachidonil glycerol, arachidonic acid and CrMP (chromium
475 mesoporphyrin) and ADVASEP-7 were purchased from Sigma-Aldrich (Missouri,
476 USA). Thapsigargin and tetrodotoxin (TTX) were purchased from Wako Pure Chemical
477 Industries (Osaka, Japan). Dantrolen was purchased from Alomone labs (Jerusalem,
478 Israel). BAPTA-AM and O,O'-Bis(2-aminoethyl)ethyleneglycol-N,N,N',N'-tetraacetic
479 acid (EGTA) were purchased from Dojindo lab (Kumamoto, Japan). FFN511 was
480 purchased from Abcam (Cambridge, England). Papain was purchased from Worthington
481 Biochemical Corporation (New Jersey, USA). RU486 was dissolved in ethanol,
482 butaclamol was dissolved in DMSO, L-NAME and SCH23390 were dissolved in water,
483 CrMP was dissolved in 0.5% 2-aminoethanol and 2 mM HCl. Oxy-hemoCD was
484 reduced in sodium dithionite and purified using a HiTrap Desalting column (GE
485 Healthcare Japan, Tokyo, Japan) and eluted in PBS. The concentration of purified
486 oxy-hemoCD is estimated by absorbance at 422 nm (Kitagishi et al., 2010). COP-1 and
487 CORM-3 were prepared according to previous publications (Clark et al., 2003; Michel

488 et al., 2012). Both reagents were stored at -20 °C and dissolved in DMSO before use.
489 For RU486 treatment, dissolved RU486 was mixed in fly food. Flies were fed RU486
490 for 5 days prior to brain preparation. Other chemicals were treated as described in the
491 main text and figure legends.
492
493 **Statistics**
494 Statistical analyses were performed using Prism software (GraphPad Software, Inc., La
495 Jolla, CA, USA) or XLtoolbox (Free Software Foundation, Inc. MA, USA). All data in
496 bar and line graphs are expressed as means ± SEMs. Student's t-test was used to
497 evaluate the statistical significance between two data sets. For multiple comparisons,
498 one-way or two-way ANOVA followed by Bonferroni post hoc analyses were employed.
499 Statistical significances are shown as *P < 0.05, **P < 0.01. P values greater than 0.05
500 were considered not statistically significant, NS > 0.05.
501
502 **SUPPLEMENTAL INFORMATION**
503 Supplemental Information includes Supplemental Experimental Procedures, three
504 supplemental figures and one supplemental Table.
505
506 **Acknowledgments**
507 This work was supported by grants from the Japanese Society for the Promotion of
508 Science (21700376, 23700405 and 25430029) to KU, and by a Grant-in-Aid for
509 Scientific Research in Innovative Areas "Memory dynamism" (25115006) to MS. We
510 thank A. Nose for *UAS-R-GECO1* transgenic flies, and T. Miyashita, M. Matsuno, T.
511 Ueno and Y. Hirano for helpful discussions. The authors declare no competing financial

interests.

Author contribution

K.U. and M.S. designed the experiments. K.U. performed most imaging experiments with K.O., S.N., and E.S. CO scavenger was synthesized by A.M., and H.K. CO probe was synthesized by J.M., and C.C. The manuscript was written by M.S. and J.H. with K.U.

521 **REFERENCES**

522 Agnati, L.F., Zoli, M., Stromberg, I., and Fuxe, K. (1995). Intercellular
523 communication in the brain: wiring versus volume transmission. Neuroscience
524 *69*, 711-726.

525 Akalal, D.B., Yu, D., and Davis, R.L. (2011). The long-term memory trace formed
526 in the Drosophila alpha/beta mushroom body neurons is abolished in long-term
527 memory mutants. J Neurosci *31*, 5643-5647.

528 Aki, T., Unuma, K., Noritake, K., Kurahashi, H., Funakoshi, T., and Uemura, K.
529 (2018). Interaction of carbon monoxide-releasing ruthenium carbonyl CORM-3
530 with plasma fibronectin. Toxicol In Vitro *50*, 201-209.

531 Alkadhi, K.A., Al-Hijailan, R.S., Malik, K., and Hogan, Y.H. (2001). Retrograde
532 carbon monoxide is required for induction of long-term potentiation in rat
533 superior cervical ganglion. J Neurosci *21*, 3515-3520.

534 Aso, Y., Grubel, K., Busch, S., Friedrich, A.B., Siwanowicz, I., and Tanimoto, H.
535 (2009). The mushroom body of adult Drosophila characterized by GAL4 drivers.
536 J Neurogenet *23*, 156-172.

537 Astort, F., Repetto, E.M., Rocha-Viegas, L., Mercau, M.E., Puch, S.S.,
538 Finkielstein, C.V., Pecci, A., and Cymeryng, C.B. (2016). Role of CREB on heme
539 oxygenase-1 induction in adrenal cells: involvement of the PI3K pathway. J Mol
540 Endocrinol *57*, 113-124.

541 Augustine, G.J., Charlton, M.P., and Smith, S.J. (1985). Calcium entry and
542 transmitter release at voltage-clamped nerve terminals of squid. J Physiol *367*,
543 163-181.

544 Balaban, P.M., Roshchin, M., Timoshenko, A.K., Gainutdinov, K.L., Bogodvid,
545 T.K., Muranova, L.N., Zuzina, A.B., and Korshunova, T.A. (2014). Nitric oxide is
546 necessary for labilization of a consolidated context memory during
547 reconsolidation in terrestrial snails. The European journal of neuroscience *40*,
548 2963-2970.

549 Balschun, D., Wolfer, D.P., Bertocchini, F., Barone, V., Conti, A., Zuschratter, W.,
550 Missiaen, L., Lipp, H.P., Frey, J.U., and Sorrentino, V. (1999). Deletion of the
551 ryanodine receptor type 3 (RyR3) impairs forms of synaptic plasticity and spatial
552 learning. The EMBO journal *18*, 5264-5273.

553 Bardo, S., Cavazzini, M.G., and Emptage, N. (2006). The role of the
554 endoplasmic reticulum Ca2+ store in the plasticity of central neurons. Trends
555 Pharmacol Sci *27*, 78-84.

556 Boehning, D., Moon, C., Sharma, S., Hurt, K.J., Hester, L.D., Ronnett, G.V.,
557 Shugar, D., and Snyder, S.H. (2003). Carbon monoxide neurotransmission
558 activated by CK2 phosphorylation of heme oxygenase-2. Neuron *40*, 129-137.

559 Boehning, D., Sedaghat, L., Sedlak, T.W., and Snyder, S.H. (2004). Heme
560 oxygenase-2 is activated by calcium-calmodulin. J Biol Chem *279*,
561 30927-30930.

562 Boultadakis, A., and Pitsikas, N. (2010). Effects of the nitric oxide synthase
563 inhibitor L-NAME on recognition and spatial memory deficits produced by
564 different NMDA receptor antagonists in the rat. Neuropsychopharmacology :
565 official publication of the American College of Neuropsychopharmacology *35*,
566 2357-2366.

567 Cervantes-Sandoval, I., Phan, A., Chakraborty, M., and Davis, R.L. (2017).
568 Reciprocal synapses between mushroom body and dopamine neurons form a
569 positive feedback loop required for learning. Elife *6*.

570 Clark, J.E., Naughton, P., Shurey, S., Green, C.J., Johnson, T.R., Mann, B.E.,
571 Foresti, R., and Motterlini, R. (2003). Cardioprotective actions by a water-soluble
572 carbon monoxide-releasing molecule. Circ Res *93*, e2-8.

573 Cui, L., Yoshioka, Y., Suyari, O., Kohno, Y., Zhang, X., Adachi, Y., Ikehara, S.,
574 Yoshida, T., Yamaguchi, M., and Taketani, S. (2008). Relevant expression of
575 Drosophila heme oxygenase is necessary for the normal development of insect
576 tissues. Biochem Biophys Res Commun *377*, 1156-1161.

577 Cypionka, H., and Meyer, O. (1983). Carbon monoxide-insensitive respiratory
578 chain of Pseudomonas carboxydovorans. J Bacteriol *156*, 1178-1187.

579 Davis, R.L. (2011). Traces of Drosophila memory. Neuron *70*, 8-19.

580 Diao, F., Ironfield, H., Luan, H., Diao, F., Shropshire, W.C., Ewer, J., Marr, E.,
581 Potter, C.J., Landgraf, M., and White, B.H. (2015). Plug-and-play genetic access
582 to drosophila cell types using exchangeable exon cassettes. Cell Rep *10*,
583 1410-1421.

584 Dubnau, J., Grady, L., Kitamoto, T., and Tully, T. (2001). Disruption of
585 neurotransmission in Drosophila mushroom body blocks retrieval but not
586 acquisition of memory. Nature *411*, 476-480.

587 Dura, J.M., Preat, T., and Tully, T. (1993). Identification of linotte, a new gene
588 affecting learning and memory in Drosophila melanogaster. J Neurogenet *9*,
589 1-14.

590 Durante, W., Christodoulides, N., Cheng, K., Peyton, K.J., Sunahara, R.K., and
591 Schafer, A.I. (1997). cAMP induces heme oxygenase-1 gene expression and
592 carbon monoxide production in vascular smooth muscle. Am J Physiol *273*,
593 H317-323.

594 Endo, M. (2009). Calcium-induced calcium release in skeletal muscle. Physiol
595 Rev *89*, 1153-1176.

596 Friggi-Grelin, F., Coulom, H., Meller, M., Gomez, D., Hirsh, J., and Birman, S.
597 (2003). Targeted gene expression in Drosophila dopaminergic cells using
598 regulatory sequences from tyrosine hydroxylase. J Neurobiol *54*, 618-627.

599 Giannini, G., Conti, A., Mammarella, S., Scrobogna, M., and Sorrentino, V.
600 (1995). The ryanodine receptor/calcium channel genes are widely and
601 differentially expressed in murine brain and peripheral tissues. The Journal of
602 cell biology *128*, 893-904.

603 Goncharenko, K., Eftekharpour, E., Velumian, A.A., Carlen, P.L., and Fehlings,

604 M.G. (2014). Changes in gap junction expression and function following
605 ischemic injury of spinal cord white matter. J Neurophysiol *112*, 2067-2075.

606 Gu, H., and O'Dowd, D.K. (2007). Whole cell recordings from brain of adult
607 Drosophila. J Vis Exp, 248.

608 Gubernator, N.G., Zhang, H., Staal, R.G., Mosharov, E.V., Pereira, D.B., Yue, M.,
609 Balsanek, V., Vadola, P.A., Mukherjee, B., Edwards, R.H.*, et al.* (2009).
610 Fluorescent false neurotransmitters visualize dopamine release from individual
611 presynaptic terminals. Science *324*, 1441-1444.

612 Hanbauer, I., Wink, D., Osawa, Y., Edelman, G.M., and Gally, J.A. (1992). Role
613 of nitric oxide in NMDA-evoked release of [3H]-dopamine from striatal slices.
614 Neuroreport *3*, 409-412.

615 Hiramatsu, M., Yokoyama, S., Nabeshima, T., and Kameyama, T. (1994).
616 Changes in concentrations of dopamine, serotonin, and their metabolites
617 induced by carbon monoxide (CO) in the rat striatum as determined by in vivo
618 microdialysis. Pharmacol Biochem Behav *48*, 9-15.

619 Huang, G., Chen, S., Li, S., Cha, J., Long, C., Li, L., He, Q., and Liu, Y. (2007).
620 Protein kinase A and casein kinases mediate sequential phosphorylation events
621 in the circadian negative feedback loop. Genes Dev *21*, 3283-3295.

622 Huang, Y.Y., and Kandel, E.R. (1995). D1/D5 receptor agonists induce a protein
623 synthesis-dependent late potentiation in the CA1 region of the hippocampus.
624 Proc Natl Acad Sci U S A *92*, 2446-2450.

625 Ichinose, T., Aso, Y., Yamagata, N., Abe, A., Rubin, G.M., and Tanimoto, H.
626 (2015). Reward signal in a recurrent circuit drives appetitive long-term memory
627 formation. Elife *4*, e10719.

628 Iliadi, K.G., Avivi, A., Iliadi, N.N., Knight, D., Korol, A.B., Nevo, E., Taylor, P.,
629 Moran, M.F., Kamyshev, N.G., and Boulianne, G.L. (2008). nemy encodes a
630 cytochrome b561 that is required for Drosophila learning and memory. Proc Natl
631 Acad Sci U S A *105*, 19986-19991.

632 Jacobitz, S., and Meyer, O. (1989). Removal of CO dehydrogenase from
633 Pseudomonas carboxydovorans cytoplasmic membranes, rebinding of CO
634 dehydrogenase to depleted membranes, and restoration of respiratory activities.
635 J Bacteriol *171*, 6294-6299.

636 Jay, T.M. (2003). Dopamine: a potential substrate for synaptic plasticity and
637 memory mechanisms. Progress in neurobiology *69*, 375-390.

638 Kakizawa, S. (2013). Nitric Oxide-Induced Calcium Release: Activation of Type 1
639 Ryanodine Receptor, a Calcium Release Channel, through Non-Enzymatic
640 Post-Translational Modification by Nitric Oxide. Front Endocrinol (Lausanne) *4*,
641 142.

642 Kakizawa, S., Yamazawa, T., Chen, Y., Ito, A., Murayama, T., Oyamada, H.,
643 Kurebayashi, N., Sato, O., Watanabe, M., Mori, N.*, et al.* (2012). Nitric
644 oxide-induced calcium release via ryanodine receptors regulates neuronal
645 function. The EMBO journal *31*, 417-428.

646 Katz, B., and Miledi, R. (1967). Ionic requirements of synaptic transmitter
647 release. Nature *215*, 651.

648 Kay, A.R., Alfonso, A., Alford, S., Cline, H.T., Holgado, A.M., Sakmann, B.,
649 Snitsarev, V.A., Stricker, T.P., Takahashi, M., and Wu, L.G. (1999). Imaging
650 synaptic activity in intact brain and slices with FM1-43 in C. elegans, lamprey,
651 and rat. Neuron *24*, 809-817.

652 Kijima, Y., Ogunbunmi, E., and Fleischer, S. (1991). Drug action of thapsigargin
653 on the Ca2+ pump protein of sarcoplasmic reticulum. The Journal of biological
654 chemistry *266*, 22912-22918.

655 Kitagishi, H., Negi, S., Kiriyama, A., Honbo, A., Sugiura, Y., Kawaguchi, A.T., and
656 Kano, K. (2010). A diatomic molecule receptor that removes CO in a living
657 organism. Angew Chem Int Ed Engl *49*, 1312-1315.

658 Kitamoto, T. (2001). Conditional modification of behavior in Drosophila by
659 targeted expression of a temperature-sensitive shibire allele in defined neurons.

660 J Neurobiol *47*, 81-92.

661 Korshunova, T.A., and Balaban, P.M. (2014). Nitric oxide is necessary for
662 long-term facilitation of synaptic responses and for development of context
663 memory in terrestrial snails. Neuroscience *266*, 127-135.

664 Lanner, J.T., Georgiou, D.K., Joshi, A.D., and Hamilton, S.L. (2010). Ryanodine
665 receptors: structure, expression, molecular details, and function in calcium
666 release. Cold Spring Harb Perspect Biol *2*, a003996.

667 Lee, J.H., Lee, S., and Kim, J.H. (2016). Amygdala Circuits for Fear Memory: A
668 Key Role for Dopamine Regulation. Neuroscientist.

669 Liu, C., Kershberg, L., Wang, J., Schneeberger, S., and Kaeser, P.S. (2018).
670 Dopamine Secretion Is Mediated by Sparse Active Zone-like Release Sites. Cell
671 *172*, 706-718 e715.

672 Lonart, G., Cassels, K.L., and Johnson, K.M. (1993). Nitric oxide induces
673 calcium-dependent [3H]dopamine release from striatal slices. J Neurosci Res *35*,
674 192-198.

675 Lu, Y.F., and Hawkins, R.D. (2002). Ryanodine receptors contribute to
676 cGMP-induced late-phase LTP and CREB phosphorylation in the hippocampus.
677 J Neurophysiol *88*, 1270-1278.

678 Mao, Z., and Davis, R.L. (2009). Eight different types of dopaminergic neurons
679 innervate the Drosophila mushroom body neuropil: anatomical and physiological
680 heterogeneity. Front Neural Circuits *3*, 5.

681 Mao, Z., Roman, G., Zong, L., and Davis, R.L. (2004). Pharmacogenetic rescue
682 in time and space of the rutabaga memory impairment by using Gene-Switch.
683 Proc Natl Acad Sci U S A *101*, 198-203.

684 Maruyama, T., Kanaji, T., Nakade, S., Kanno, T., and Mikoshiba, K. (1997).
685 2APB, 2-aminoethoxydiphenyl borate, a membrane-penetrable modulator of
686 Ins(1,4,5)P3-induced Ca2+ release. J Biochem *122*, 498-505.

687 Matsuda, W., Furuta, T., Nakamura, K.C., Hioki, H., Fujiyama, F., Arai, R., and
688 Kaneko, T. (2009). Single nigrostriatal dopaminergic neurons form widely spread
689 and highly dense axonal arborizations in the neostriatum. J Neurosci *29*,
690 444-453.

691 McGuire, S.E., Le, P.T., and Davis, R.L. (2001). The role of Drosophila
692 mushroom body signaling in olfactory memory. Science *293*, 1330-1333.

693 Meinrenken, C.J., Borst, J.G., and Sakmann, B. (2003). Local routes revisited:
694 the space and time dependence of the Ca2+ signal for phasic transmitter
695 release at the rat calyx of Held. J Physiol *547*, 665-689.

696 Michel, B.W., Lippert, A.R., and Chang, C.J. (2012). A reaction-based
697 fluorescent probe for selective imaging of carbon monoxide in living cells using a
698 palladium-mediated carbonylation. J Am Chem Soc *134*, 15668-15671.

699 Miesenbock, G., De Angelis, D.A., and Rothman, J.E. (1998). Visualizing
700 secretion and synaptic transmission with pH-sensitive green fluorescent proteins.
701 Nature *394*, 192-195.

702 Molina-Luna, K., Pekanovic, A., Rohrich, S., Hertler, B., Schubring-Giese, M.,
703 Rioult-Pedotti, M.S., and Luft, A.R. (2009). Dopamine in motor cortex is
704 necessary for skill learning and synaptic plasticity. PloS one *4*, e7082.

705 Muller, U. (1994). Ca2+/calmodulin-dependent nitric oxide synthase in Apis
706 mellifera and Drosophila melanogaster. The European journal of neuroscience *6*,
707 1362-1370.

708 Muller, U. (1996). Inhibition of nitric oxide synthase impairs a distinct form of
709 long-term memory in the honeybee, Apis mellifera. Neuron *16*, 541-549.

710 Ng, M., Roorda, R.D., Lima, S.Q., Zemelman, B.V., Morcillo, P., and Miesenbock,
711 G. (2002). Transmission of olfactory information between three populations of
712 neurons in the antennal lobe of the fly. Neuron *36*, 463-474.

713 Oyamada, T., Hayashi, T., Kagaya, A., Yokota, N., and Yamawaki, S. (1998).

714 Effect of dantrolene on K(+)- and caffeine-induced dopamine release in rat
715 striatum assessed by in vivo microdialysis. Neurochem Int *32*, 171-176.

716 Park, S.Y., Kim, J.H., Lee, S.J., and Kim, Y. (2013). Involvement of PKA and
717 HO-1 signaling in anti-inflammatory effects of surfactin in BV-2 microglial cells.
718 Toxicol Appl Pharmacol *268*, 68-78.

719 Pereira, D.B., Schmitz, Y., Meszaros, J., Merchant, P., Hu, G., Li, S., Henke, A.,
720 Lizardi-Ortiz, J.E., Karpowicz, R.J., Jr., Morgenstern, T.J.*, et al.* (2016).
721 Fluorescent false neurotransmitter reveals functionally silent dopamine vesicle
722 clusters in the striatum. Nat Neurosci *19*, 578-586.

723 Pfeiffer, B.D., Truman, J.W., and Rubin, G.M. (2012). Using translational
724 enhancers to increase transgene expression in Drosophila. Proc Natl Acad Sci U
725 S A *109*, 6626-6631.

726 Poss, K.D., Thomas, M.J., Ebralidze, A.K., O'Dell, T.J., and Tonegawa, S. (1995).
727 Hippocampal long-term potentiation is normal in heme oxygenase-2 mutant
728 mice. Neuron *15*, 867-873.

729 Puig, M.V., Antzoulatos, E.G., and Miller, E.K. (2014). Prefrontal dopamine in
730 associative learning and memory. Neuroscience *282*, 217-229.

731 Regehr, W.G., Carey, M.R., and Best, A.R. (2009). Activity-dependent regulation
732 of synapses by retrograde messengers. Neuron *63*, 154-170.

733 Regulski, M., and Tully, T. (1995). Molecular and biochemical characterization of
734 dNOS: a Drosophila Ca2+/calmodulin-dependent nitric oxide synthase. Proc
735 Natl Acad Sci U S A *92*, 9072-9076.

736 Rice, M.E., and Cragg, S.J. (2008). Dopamine spillover after quantal release:
737 rethinking dopamine transmission in the nigrostriatal pathway. Brain research
738 reviews *58*, 303-313.

739 Rorig, B., Klausa, G., and Sutor, B. (1996). Intracellular acidification reduced gap
740 junction coupling between immature rat neocortical pyramidal neurones. J

741 Physiol *490 (Pt 1)*, 31-49.

742 Sabatini, B.L., and Regehr, W.G. (1996). Timing of neurotransmission at fast
743 synapses in the mammalian brain. Nature *384*, 170-172.

744 Sacca, G.B., Saenz, D.A., Jaliffa, C.O., Minces, L., Keller Sarmiento, M.I., and
745 Rosenstein, R.E. (2003). Photic regulation of heme oxygenase activity in the
746 golden hamster retina: involvement of dopamine. J Neurochem *85*, 534-542.

747 Sagara, Y., and Inesi, G. (1991). Inhibition of the sarcoplasmic reticulum Ca2+
748 transport ATPase by thapsigargin at subnanomolar concentrations. The Journal
749 of biological chemistry *266*, 13503-13506.

750 Shibuki, K., Kimura, S., and Wakatsuki, H. (2001). Suppression of the induction
751 of long-term depression by carbon monoxide in rat cerebellar slices. The
752 European journal of neuroscience *13*, 609-616.

753 Stewart, B.A., Atwood, H.L., Renger, J.J., Wang, J., and Wu, C.F. (1994).
754 Improved stability of Drosophila larval neuromuscular preparations in
755 haemolymph-like physiological solutions. J Comp Physiol A *175*, 179-191.

756 Stone, J.R., and Marletta, M.A. (1994). Soluble guanylate cyclase from bovine
757 lung: activation with nitric oxide and carbon monoxide and spectral
758 characterization of the ferrous and ferric states. Biochemistry *33*, 5636-5640.

759 Sugimura, Y., Yoshizaki, F., Katagiri, J., and Horiuchi, C. (1980). Studies on algal
760 cytochromes. I. Purification and properties of cytochrome b-561 from
761 Enteromorpha prolifera. J Biochem *87*, 541-547.

762 Takasago, T., Imagawa, T., Furukawa, K., Ogurusu, T., and Shigekawa, M.
763 (1991). Regulation of the cardiac ryanodine receptor by protein
764 kinase-dependent phosphorylation. J Biochem *109*, 163-170.

765 Takemura, S.Y., Aso, Y., Hige, T., Wong, A., Lu, Z., Xu, C.S., Rivlin, P.K., Hess,
766 H.F., Zhao, T., Parag, T.*, et al.* (2017). A connectome of a learning and memory
767 center in the adult Drosophila brain. Elife *6*.

768 Tamura, T., Chiang, A.S., Ito, N., Liu, H.P., Horiuchi, J., Tully, T., and Saitoe, M.
769 (2003). Aging specifically impairs amnesiac-dependent memory in Drosophila.
770 Neuron *40*, 1003-1011.

771 Taskiran, D., Kutay, F.Z., and Pogun, S. (2003). Effect of carbon monoxide on
772 dopamine and glutamate uptake and cGMP levels in rat brain.
773 Neuropsychopharmacology : official publication of the American College of
774 Neuropsychopharmacology *28*, 1176-1181.

775 Tenhunen, R., Marver, H.S., and Schmid, R. (1969). Microsomal heme
776 oxygenase. Characterization of the enzyme. The Journal of biological chemistry
777 *244*, 6388-6394.

778 Tinajero-Trejo, M., Denby, K.J., Sedelnikova, S.E., Hassoubah, S.A., Mann, B.E.,
779 and Poole, R.K. (2014). Carbon monoxide-releasing molecule-3 (CORM-3;
780 Ru(CO)3Cl(glycinate)) as a tool to study the concerted effects of carbon
781 monoxide and nitric oxide on bacterial flavohemoglobin Hmp: applications and
782 pitfalls. J Biol Chem *289*, 29471-29482.

783 Tully, T., and Quinn, W.G. (1985). Classical conditioning and retention in normal
784 and mutant Drosophila melanogaster. J Comp Physiol A *157*, 263-277.

785 Ueno, K., Naganos, S., Hirano, Y., Horiuchi, J., and Saitoe, M. (2013). Long-term
786 enhancement of synaptic transmission between antennal lobe and mushroom
787 body in cultured Drosophila brain. J Physiol *591*, 287-302.

788 Ueno, K., Suzuki, E., Naganos, S., Ofusa, K., Horiuchi, J., and Saitoe, M. (2017).
789 Coincident postsynaptic activity gates presynaptic dopamine release to induce
790 plasticity in Drosophila mushroom bodies. Elife *6*.

791 Verkhratsky, A. (2005). Physiology and pathophysiology of the calcium store in
792 the endoplasmic reticulum of neurons. Physiol Rev *85*, 201-279.

793 Vreman, H.J., Ekstrand, B.C., and Stevenson, D.K. (1993). Selection of
794 metalloporphyrin heme oxygenase inhibitors based on potency and
795 photoreactivity. Pediatric research *33*, 195-200.

Wan, K., Moriya, T., Akiyama, M., Takeshima, H., and Shibata, S. (1999). Involvement of ryanodine receptor type 3 in dopamine release from the striatum: evidence from mutant mice lacking this receptor. Biochem Biophys Res Commun *266*, 588-592.

Wang, R., and Wu, L. (2003). Interaction of selective amino acid residues of K(ca) channels with carbon monoxide. Exp Biol Med (Maywood) *228*, 474-480.

Wang, Y., Mamiya, A., Chiang, A.S., and Zhong, Y. (2008). Imaging of an early memory trace in the Drosophila mushroom body. J Neurosci *28*, 4368-4376.

Wang, Y., Wu, J., Rowan, M.J., and Anwyl, R. (1996). Ryanodine produces a low frequency stimulation-induced NMDA receptor-independent long-term potentiation in the rat dentate gyrus in vitro. J Physiol *495 (Pt 3)*, 755-767.

Xu, L., Eu, J.P., Meissner, G., and Stamler, J.S. (1998). Activation of the cardiac calcium release channel (ryanodine receptor) by poly-S-nitrosylation. Science *279*, 234-237.

Yagishita, S., Hayashi-Takagi, A., Ellis-Davies, G.C., Urakubo, H., Ishii, S., and Kasai, H. (2014). A critical time window for dopamine actions on the structural plasticity of dendritic spines. Science *345*, 1616-1620.

Yamasaki, M., and Takeuchi, T. (2017). Locus Coeruleus and Dopamine-Dependent Memory Consolidation. Neural plasticity *2017*, 8602690.

Yu, D., Akalal, D.B., and Davis, R.L. (2006). Drosophila alpha/beta mushroom body neurons form a branch-specific, long-term cellular memory trace after spaced olfactory conditioning. Neuron *52*, 845-855.

Zalk, R., Lehnart, S.E., and Marks, A.R. (2007). Modulation of the ryanodine receptor and intracellular calcium. Annu Rev Biochem *76*, 367-385.

Zhao, F., Li, P., Chen, S.R., Louis, C.F., and Fruen, B.R. (2001). Dantrolene inhibition of ryanodine receptor Ca2+ release channels. Molecular mechanism and isoform selectivity. The Journal of biological chemistry *276*, 13810-13816.

Zhu, X.Z., and Luo, L.G. (1992). Effect of nitroprusside (nitric oxide) on endogenous dopamine release from rat striatal slices. J Neurochem *59*, 932-935.

Zhuo, M., Small, S.A., Kandel, E.R., and Hawkins, R.D. (1993). Nitric oxide and carbon monoxide produce activity-dependent long-term synaptic enhancement in hippocampus. Science *260*, 1946-1950.

Zorzato, F., Scutari, E., Tegazzin, V., Clementi, E., and Treves, S. (1993). Chlorocresol: an activator of ryanodine receptor-mediated Ca2+ release. Mol Pharmacol *44*, 1192-1201.

833 **Figures and legends**

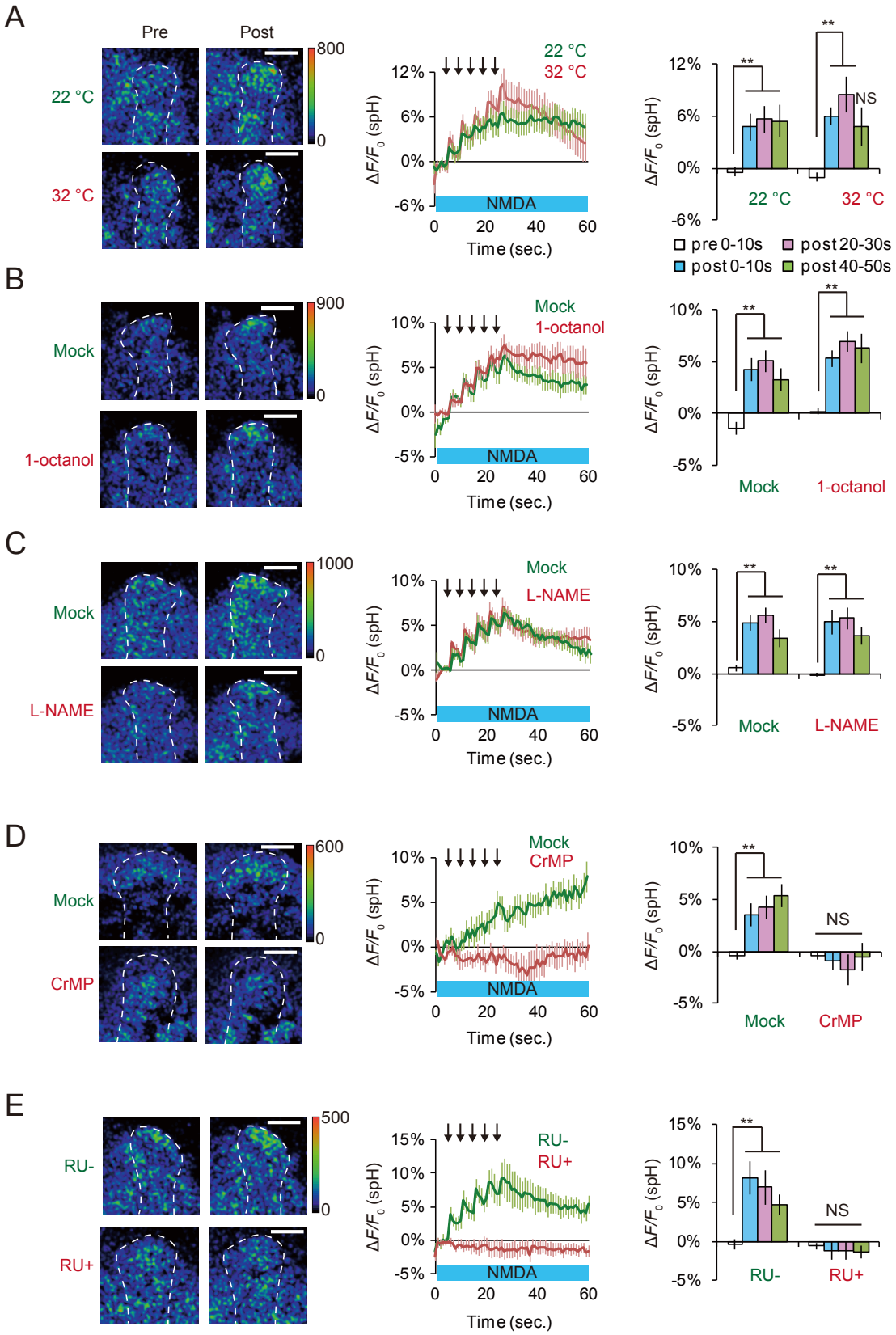

834

835 **Figure 1. Inhibiting heme oxygenase (HO) activity in the MBs blocks SV exocytosis**
836 **from pre-synaptic DA terminals**

837 (A) Blocking SV exocytosis from the MBs does not affect DA release. spH fluorescence
838 was measured at TH-DA terminals innervating the tip of the MB vertical lobes of
839 *MB-LexA>LexAop-shi*^{ts} brain. (Left) typical pseudo color images 5 s before and 30 s
840 after coincident AL + NMDA activation. (Middle) time course of fluorescent changes,
841 and (right) summary graphs. One-way ANOVA and post hoc tests indicate significant
842 changes in fluorescence at both restrictive ($F_{3,32}$ = 6.137, P = 0.002) and permissive
843 ($F_{3,32}$ = 4.003, P = 0.016) temperatures. N = 9 for all data. Scale bars = 20 μm.

844 (B) The gap junction inhibitor, 1-octanol, does not affect DA release. One-way ANOVA
845 and post hoc tests indicate significant fluorescence changes in both 1 mM octanol
846 treated ($F_{3,28}$ = 10.323, P < 0.001, N = 8) and in mock treated ($F_{3,32}$ = 9.723, P < 0.001,
847 N = 9) groups.

848 (C) The NOS inhibitor, L-NAME, does not affect SV exocytosis from TH-DA terminals.
849 One-way ANOVA and post hoc tests indicate significant changes in both 100 μM
850 L-NAME treated ($F_{3,24}$ = 8.432, P = 0.001, N = 7) and mock treated ($F_{3,28}$ = 10.552, P <
851 0.001, N = 8) groups.

852 (D) The HO inhibitor, CrMP, prevents DA release. One-way ANOVA and post hoc tests
853 indicate significant DA release after mock treatment ($F_{3,32}$ = 5.858, P = 0.003, N = 9),
854 but not after treatment with 10 μM CrMP ($F_{3,36}$ = 0.300, P = 0.825, N = 10).

855 (E) *dHO* knockdown in the MBs prevents DA release. One-way ANOVA and post hoc
856 tests identify significant DA release upon coincident stimulation when *dHO-IR* is not
857 expressed (RU-) ($F_{3,36}$= 4.685, P = 0.007). This release is abolished in the
858 RNAi-induced (RU+) group ($F_{3,36}$= 0.141, P = 0.935). N = 10 for all data.

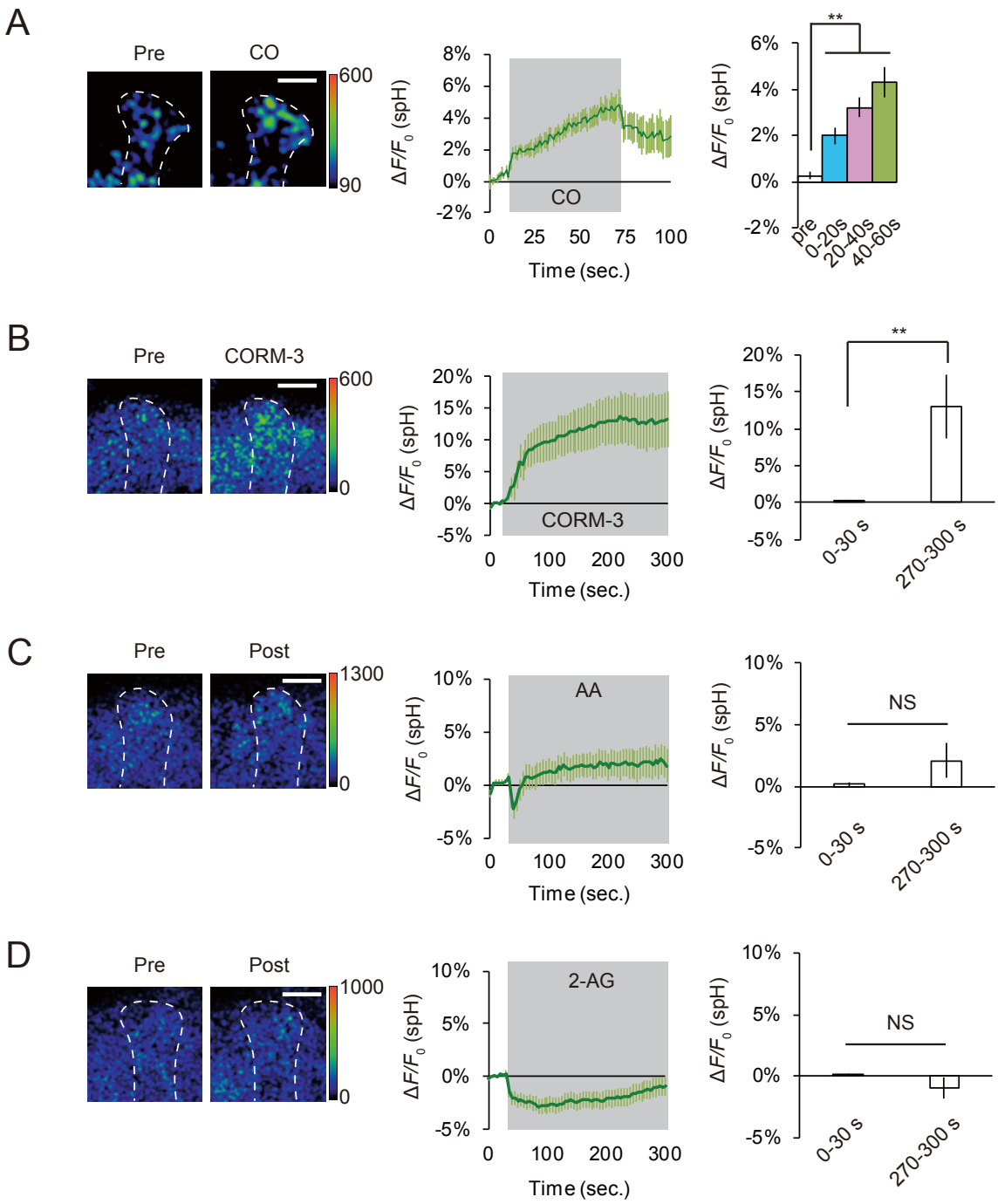

Figure 2. CO evokes SV exocytosis from DA terminals

(A) CO induces DA release. CO-saturated saline was puffed onto the vertical lobes of the MB during the indicated time period (gray-shaded area in the middle panel). CO-induced spH responses were obtained by subtracting spH fluorescent changes induced by control N_2-satulated saline from fluorescence changes induced by

865 CO-saturated saline. One-way ANOVA and post hoc tests indicate significant changes
866 in spH fluorescence upon CO application ($F_{3,44}$= 14.994, P < 0.001). N = 12 for all data.
867 (B) CORM-3 induces DA release. 20 μM CORM-3 (dissolved in 0.2% DMSO) was
868 bath applied and spH fluorescence was measured at DA terminals at the tip of the MB
869 vertical lobes. CORM-3 induced spH responses were obtained by subtracting
870 fluorescent changes induced by control 0.2% DMSO saline from fluorescence changes
871 induced by CORM-3. ** P < 0.01 determined by Student's t-test, comparing spH
872 responses before (0-30s) and after application of CO (270-300s). N = 8 for all data.
873 (C) Arachidonic acid (AA) does not induce DA release. 200 μM AA (dissolved in 0.4 %
874 ethanol) was bath applied. AA-induced spH responses were obtained by subtracting
875 fluorescence changes induced by 0.4% ethanol saline from fluorescence changes
876 induced by AA. NS P > 0.05 by Student's t-test and N = 16 for all data.
877 (D) Effects of 2-arachidonylglycerol (2-AG) on DA release. Bath application of 200
878 μM AG (dissolved in 0.2 % DMSO) did not induce SV exocytosis in TH-DA terminals.
879 AG-induced spH responses were obtained by subtracting fluorescence changes induced
880 by 0.2% DMSO saline from fluorescence changes induced by AG. NS P > 0.05
881 determined by Student's t-test. N = 12 for all data.

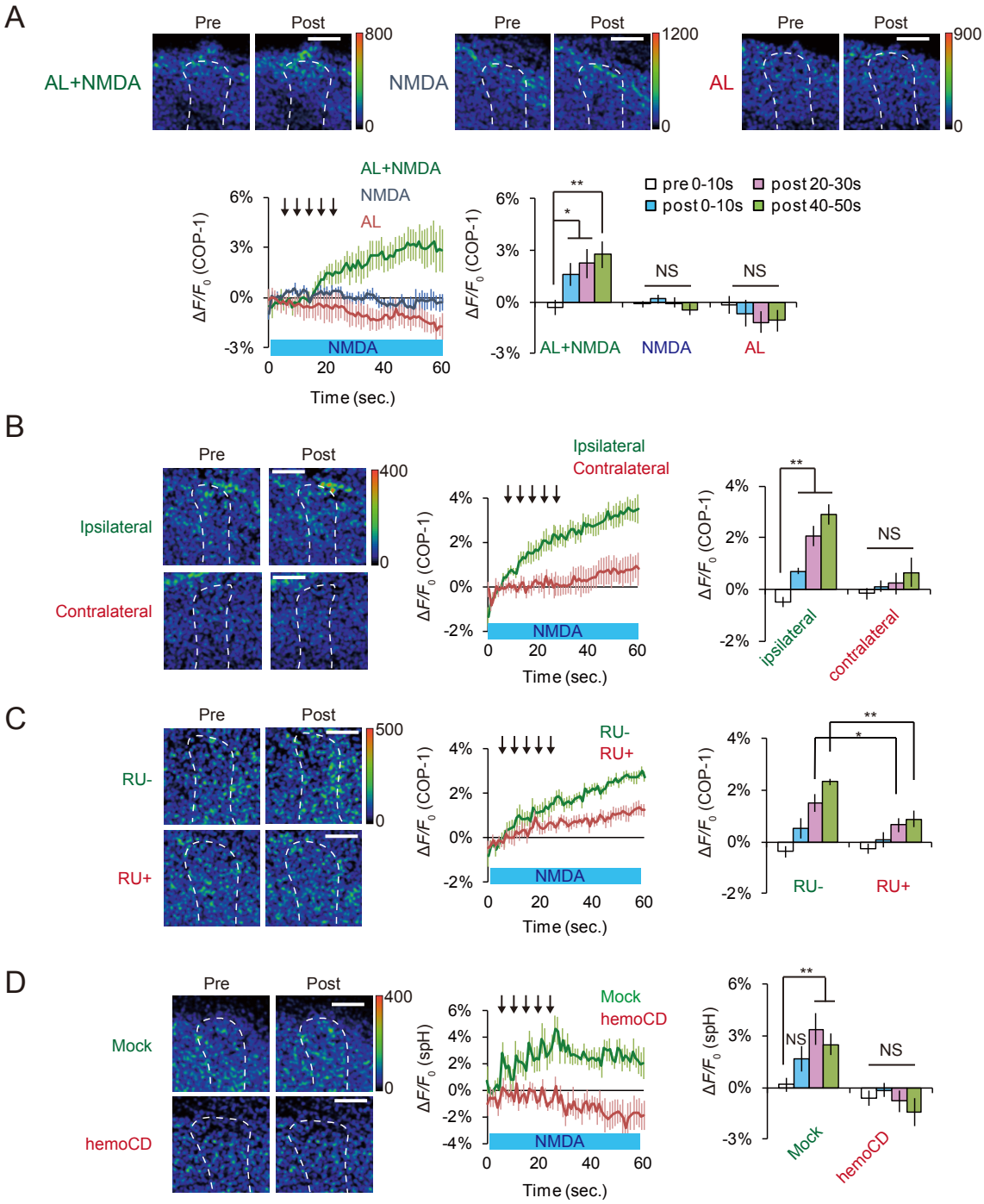

882

883 **Figure 3. Endogenous CO released from MBs induces DA release**

884 (A) Top panels, typical images of COP-1 fluorescence observed at the tips of the MB

885 vertical lobes. Pre refers to images taken prior to stimulation, while Post refers to

886 images taken 30 secs after onset of indicated stimuli. Lower left, time course of COP-1

887 fluorescence upon indicated stimulation protocols, and lower right, summary of COP-1
888 fluorescence at different time intervals upon indicated stimulation. Isolated brains were
889 soaked in 4 μM COP-1, and COP-1 responses were calculated by subtracting
890 non-stimulated fluorescence changes from stimulated fluorescence changes. One-way
891 ANOVA and post hoc tests indicate significant changes in fluorescence after AL +
892 NMDA stimulation ($F_{3,24}$= 3.787, P = 0.023, N = 7), but not after NMDA ($F_{3,28}$= 0.743,
893 P = 0.534, N = 8) or AL stimulation alone ($F_{3,28}$= 0.518, P = 0.674, N = 8). Scale bars =
894 20 μm
895 (B) CO is released from the MB lobe ipsilateral to AL stimulation. One-way ANOVA
896 and post hoc tests indicate significant changes in COP-1 fluorescence in MB lobes
897 ipsilateral ($F_{3,32}$= 23.816, P < 0.001) to the AL lobe stimulated during AL + NMDA
898 stimulation, but not in the contralateral lobe ($F_{3,32}$= 0.779, P = 0.514). N = 9.
899 (C) Knocking down *dHO* expression in the MBs impairs CO production. Two-way
900 ANOVA and post hoc tests indicate significant differences in COP-1 fluorescence due to
901 time, treatment (RU+ induced *dHO-IR* versus RU- uninduced), and interaction between
902 time and treatment ($F_{3,88}$= 4.137, P = 0.0086). N = 12 for all data.
903 (D) The CO scavenger, hemoCD, prevents SV exocytosis from DA terminals. AL +
904 NMDA-dependent changes in spH fluorescence were measured in the presence and
905 absence of 50 μM hemoCD. One-way ANOVA and post hoc tests indicate significant
906 changes in fluorescence upon stimulation in mock ($F_{3,28}$= 3.877, P = 0.019) but not in
907 hemoCD treated brains ($F_{3,28}$= 0.749, P = 0.532). N = 8 for all data.
908

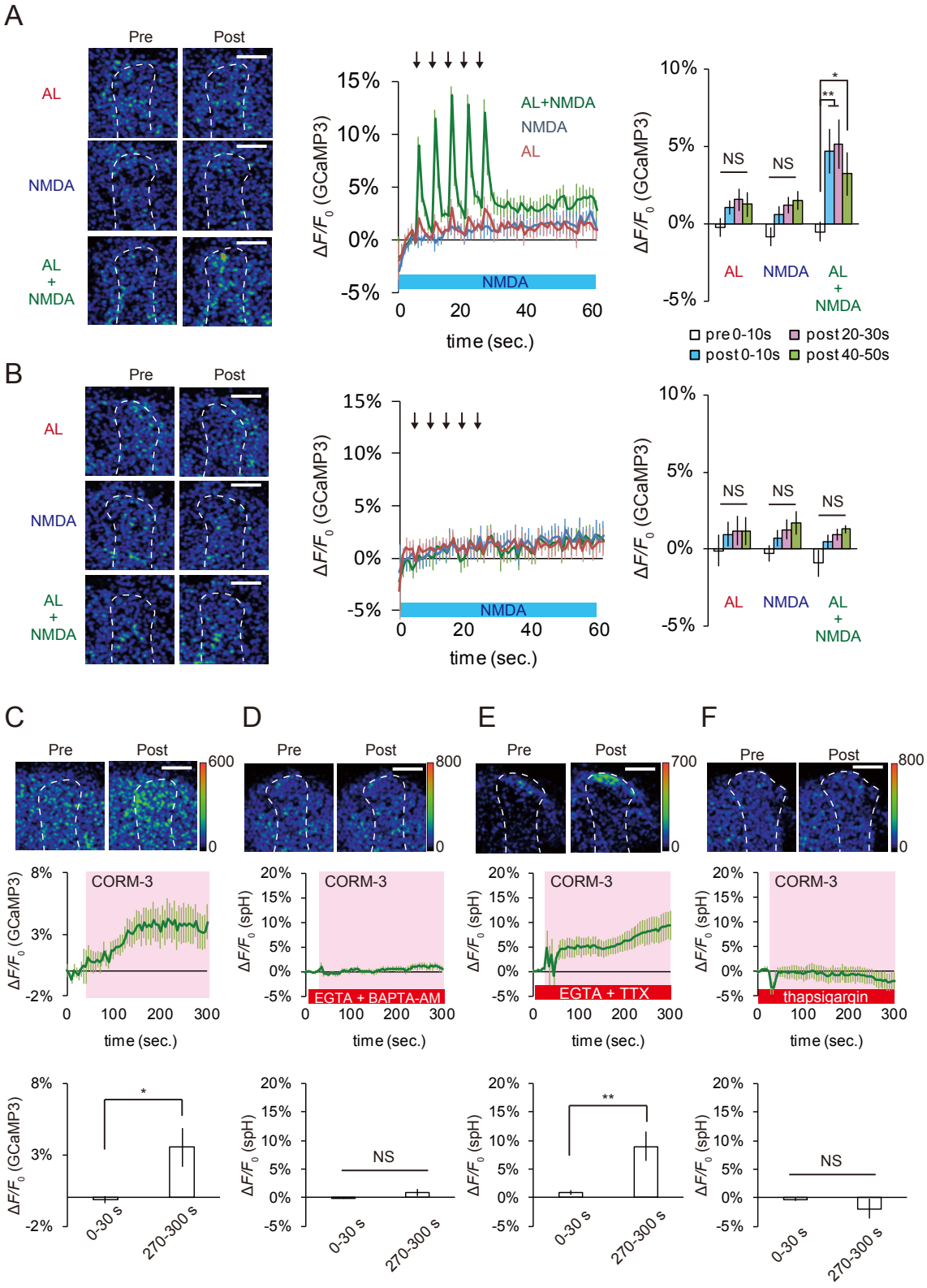

Figure 4. CO induced DA release requires Ca^{2+} efflux from internal Ca^{2+} stores.

(A) Left panel, typical pseudo color images of G-CaMP3 fluorescence in TH-DA

912 terminals innervating the tips of the vertical lobes of the MB ipsilateral to AL
913 stimulation. Stimulation type is shown on the side, and responses before (pre) and after
914 (post) stimulation are shown. Middle panel, time course of Ca^{2+} responses in TH-DA
915 terminals innervating the ipsilateral MB upon indicated stimulation. Right panel,
916 summary of responses to indicated stimuli. One-way ANOVA and post hoc tests
917 indicate significant changes in Ca^{2+} signals after AL + NMDA stimulation ($F_{3,32}$= 3.759,
918 P = 0.020) but not after NMDA ($F_{3,32}$= 1.554, P = 0.220) or AL stimulation alone
919 ($F_{3,32}$= 1.426, P = 0.253). N = 9 for all experiments.
920 (B) G-CaMP3 fluorescence changes in TH-DA terminals innervating the MB
921 contralateral to AL stimulation. Panels are similar to those shown in (A). One-way
922 ANOVA did not identify any significant changes after stimulation of the AL + NMDA
923 ($F_{3,32}$= 1.626, P = 0.203), NMDA alone ($F_{3,32}$= 1.929, P = 0.145) or AL alone ($F_{3,32}$=
924 0.709, P = 0.465). N = 9 for all data.
925 (C) CORM-3 induces Ca^{2+} increases in TH-DA terminals. CORM-3 induced Ca^{2+}
926 changes were calculated by subtracting Mock induced fluorescence changes from
927 CORM-3 induced fluorescence changes. 20 μM CORM-3 (dissolved in 0.2% DMSO
928 saline) was puffed onto the tips of the vertical MB lobes during the indicated time
929 period (shown in pink in the middle panel). P = 0.013 assayed by Student's t-test,
930 comparing Ca^{2+} changes before (0-30 s) and after (270-300 s) CORM-3 application. N
931 = 16 for all data.
932 (D) CORM-3-induced DA release depends on increases in intracellular Ca^{2+}. Brains
933 were incubated in the Ca^{2+}-free external solution containing 2 mM EGTA and 10 μM
934 BAPTA-AM for 10 min prior to CORM-3 application. P = 0.166 determined by
935 Student's t-test. N = 12.

936 (E) CORM-3-induced DA release does not require influx of external Ca^{2+} or activity of
937 voltage-gated Na^{+} channels. Brains were placed in the Ca^{2+}-free external solution
938 containing 5 mM EGTA and 10 μM TTX 10 min prior to CORM-3 application. ***P* =
939 0.0094 as determined by Student's t-test. N = 13.
940 (F) CORM-3-induced DA release requires efflux from internal Ca^{2+} stores. Brains were
941 incubated in Ca^{2+}-free external solution containing 10 μM thapsigargin for 10 min prior
942 to CORM-3 application. *P* = 0.364 determined by Student's t-test. N = 14.

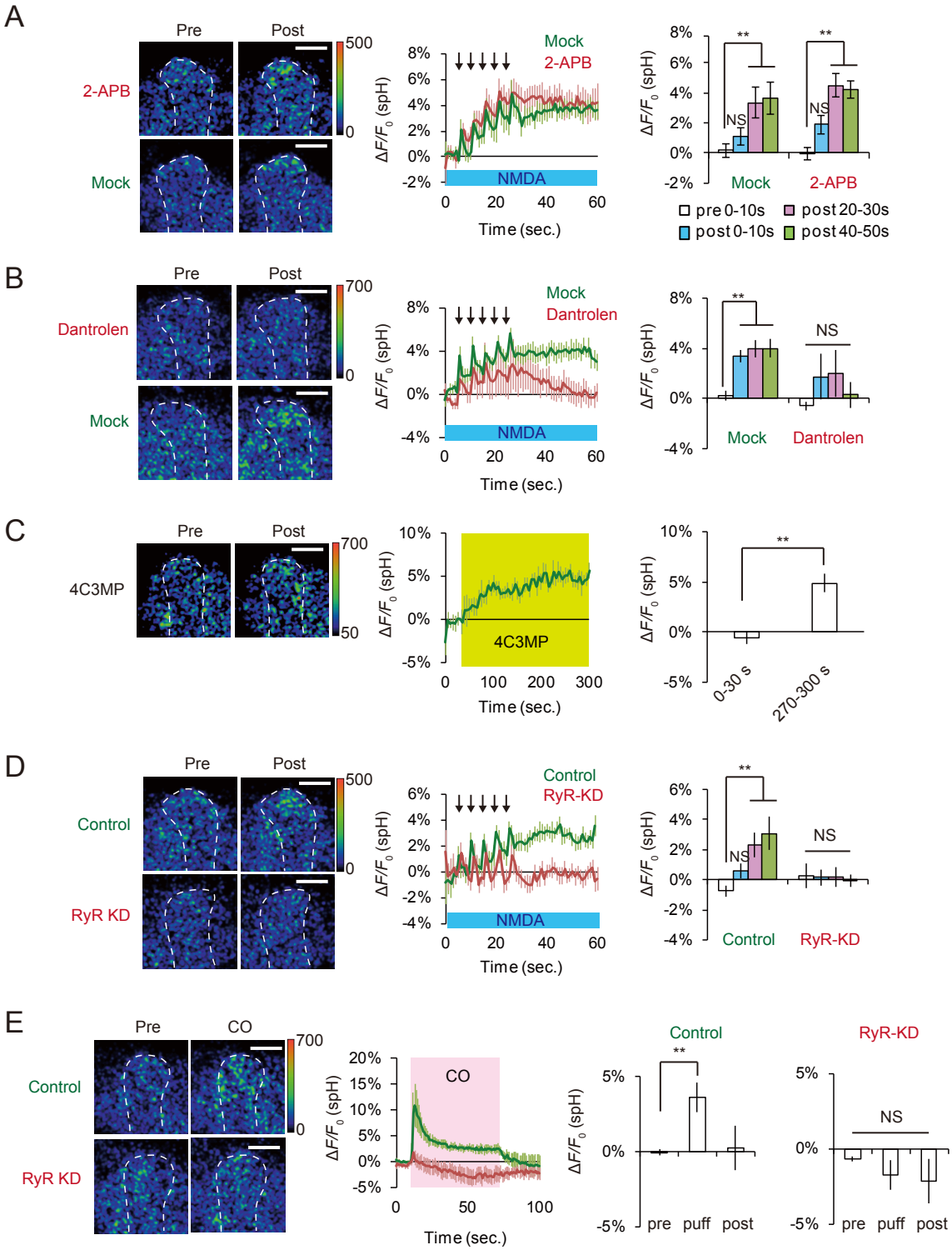

943

944 **Figure 5. CO induced DA release is mediated by ryanodine receptors.**

945 (A) An IP_3R inhibitor does not affect DA release. 100 μM

946 2-aminoethoxydiphenylborane (2-APB) was dissolved in 0.1 % DMSO saline. One-way

947 ANOVA and post hoc tests indicate significant increases in spH fluorescence upon AL +
948 NMDA stimulation in both the 2-APB treated group ($F_{3,36}$ = 7.043, P < 0.001, N = 10)
949 as well as the mock treated group ($F_{3,32}$ = 7.978, P < 0.001, N = 9).
950 (B) The RyR inhibitor, dantrolen, inhibits DA release. 10 μM dantrolen was dissolved in
951 0.1% DMSO saline. Significant increases in spH fluorescence upon AL + NMDA
952 stimulation were observed in mock treated brains ($F_{3,28}$ = 8.805, P < 0.001), while
953 dantrolen treatment suppressed this effect ($F_{3,36}$ = 0.760, P = 0.526). N = 8 for all data.
954 (C) Application of a RyR agonist induces DA release. 1 mM 4-chloro-3-methylphenol
955 (4C3MP) was dissolved in 0.2% ethanol saline containing 1 μM TTX and applied for
956 the indicated period of time (shown in yellow). ** P < 0.001 as assayed by Student's
957 t-test comparing before (0-30 s) and after (280-300 s) 4C3MP treatment. N = 8 for all
958 data.
959 (D) *RyR* knockdown in TH-DA neurons (RyR KD) prevents DA release evoked by AL +
960 NMDA stimulation. One-way ANOVA and post hoc tests indicate suppression of SV
961 exocytosis in the RyR KD group ($F_{3,28}$= 0.043, P = 0.988) in contrast to the control
962 group ($F_{3,28}$= 5.091, P = 0.006). N = 8 for all data.
963 (E) Knocking down *RyR* expression in TH-DA neurons (RyR-KD) prevents DA release
964 evoked by CO application. CO saturated saline was applied during the indicated time
965 period (shown in pink) from a micro pipet. One-way ANOVA and post hoc tests indicate
966 suppression of SV exocytosis in the RyR-KD group ($F_{2,21}$= 0.538, P = 0.592) but not in
967 the control group ($F_{2,21}$= 3.998, P = 0.034). N = 8 for all data.
968
969